UNIVERSITY OF CALIFORNIA SAN DIEGO

A possible role of the acid/base sensing enzyme soluble adenylyl cyclase (sAC) inhibition on photosynthesis in the marine diatom *Thalassiosira pseudonana*

A thesis submitted in partial satisfaction of the requirements for

the degree Master of Science

in

Marine Biology

by

Bethany L. Shimasaki

Committee in charge:

Professor Martin Tresguerres, Chair
Professor Andrew E. Allen
Professor Bianca Brahamsha

2020

The thesis of Bethany L. Shimasaki is approved, and it is acceptable in quality and form for publication on microfilm and electronically.

University of California San Diego

2020

Dedication

I would like to dedicate this thesis to family, friends, colleagues and mentors who have given me so much love, support, inspiration and wisdom throughout my life. I would especially like to give special recognition to a few individuals who have had particularly important impacts on my life.

To my mother Cindy and my father Mike, who, without them, none of what I've accomplished in life would be possible. You have given me so much of your love, your time and encouragement to keep working hard, persevere through trials, and always remember what really matters. To my brothers Evan and DG, who always know the right thing to say when I need encouragement and who always have my back. To all my aunties and uncles and cousins who made sure that I was well-fed, cared for, and supported every single week, no matter what.

To my Uncle Ron, Poh Poh, Grandma and Grandpa, who set the foundation for who I am today and taught me how to value myself, work hard, and treasure the people around me. I wish you were all here for me to share this moment with, but I hope that I'm making you proud every day.

To my SIO squad, Bryant Jew, Marelle Arndt, Michelle Prieto, and JT Terhall. To Andrew Chin, Hyejoo Ro, Christina Jayne, and Dusty Greer. Thank you for your continual support, love, encouragement, laughter, and the joy that you bring to my life.

To Christine Fong, for always supporting me, no matter what the situation, and being an absolute blessing in my life. I cannot express how thankful I am to have you as a best friend, roommate, and sister.

To the Tresguerres Lab. I would not have made it through this program without your guidance, support, encouragement, laughter and memes. Thank you!

Thank you to everyone who has had an impact on my life and made the completion of this Thesis possible. I would not have been able to accomplish anything without the support of those around me.

Table of Contents

List of Figures

List of Tables

Acknowledgements

I would like to acknowledge and thank several individuals who have been pivotal contributors of scientific knowledge, education, and mentorship in the creation of this thesis.

Martin Tresguerres, principal investigator and the chair of my thesis committee, always encouraged and challenged me to work harder, think critically, and strive for the best work that I could produce. He always provided sound advice and support throughout my thesis.

Daniel Yee, my mentor and head of "team diatom", dedicated countless amounts of his time to teach me the needed lab skills and provide me with the knowledge to succeed as a graduate student. He has taught me so much about the skills needed to be a researcher, but also the patience and dedication that are required as well. He has had seemingly infinite amounts of patience while mentoring me, which is truly inspiring.

Dovi Kacev, for the encouragement, guidance, and advice you have given me over the past year. His support has been much appreciated and always comes at the right time.

I would also like to acknowledge Andy Allen and Bianca Brahamsha for participating as members of my thesis committee. I've learned a lot from them during my time in classes they have taught and am grateful for the time and knowledge they have given me throughout this process.

ABSTRACT OF THESIS

A possible role of the acid/base sensing enzyme soluble adenylyl cyclase (sAC) inhibition on photosynthesis in the marine diatom *Thalassiosira pseudonana*

by

Bethany L. Shimasaki

Master of Science in Marine Biology

University of California San Diego, 2020

Professor Martin Tresguerres, Chair

Diatoms have evolved complex processes called carbon concentrating mechanisms (CCMs) to maintain high photosynthesis rates by accumulating CO_2 at the site of Rubisco, the key enzyme in carbon fixation. Many CCM proteins are known to be regulated in response to environmental pH, CO_2 and HCO_3^- levels *via* the cyclic adenosine monophosphate (cAMP) signaling pathway. However, the regulatory pathways are poorly understood. The goal of my thesis was to explore a potential role soluble adenylyl cyclase (sAC) has in regulating photosynthesis by the marine diatom *Thalassiosira pseudonana*. This enzyme is stimulated by

HCO_3^- to produce cAMP, and deemed an evolutionary conserved CO_2/pH/HCO_3^- sensor. Two sAC-like genes, Thaps3-24827 and Thaps3-22442, were cloned into fcp-sAC-eGFP expression vectors that add enhanced green fluorescent protein (eGFP) tag with the purpose of studying their subcellular localizations. However, this approached failed, likely due to the large size of the genes; ~6.8 for Thaps3-24827 and~5.8 kilobase pairs for Thaps3-22442. The functional role of sAC in modulating diatom photosynthesis was studied by measuring oxygen (O_2) production rates in the absence and presence of KH7, a small molecule that specifically inhibits sAC. Gross O_2 production (GOP) was inhibited by KH7 in a dose-dependent fashion, and effects were partially reversible following a washout. The degree of KH7 inhibition was variable between cultures, and 10μM inhibited GOP between ~50-90%. Additionally, 20μM KH7 affected O_2 consumption rate. These results suggest that sAC may act as a CO_2/pH/HCO_3^- sensor that regulates photosynthesis in diatoms, perhaps by modulating CCM-related proteins.

Introduction

Marine diatoms are key photosynthetic organisms, responsible for up to 40% of primary production in the ocean and producing up to 20% of primary production globally (Field et al., 1998; Falkowski et al., 2000). Their unique silica cell walls called frustules enable them to become important sources of silica in the marine environment (Yool and Tyrrell 2003) and play integral roles in the biogeochemical cycling of the ocean and food web dynamics through mechanisms like carbon fixation, iron use, nutrient flux between deep water and surface zones and photosynthesis (Falkowski et al., 1998; 2004). But despite their ecological importance, some key aspects of the mechanisms that sustain photosynthesis and how they are regulated in response to a changing environment remain poorly understood.

The enzyme soluble adenylyl cyclase (sAC) has been shown to act as a molecular CO_2/pH/HCO_3^- sensor in many aquatic animals (Tresguerres et al., 2014). There are several putative sAC-like genes in the marine diatom species *Thalassiosira pseudonana* (Tresguerres, 2014) and in *Phaeodactylum tricornutum* (Matsuda et al., 2011); however, their physiological roles remain unknown. Thus, the goal of my thesis was to explore a potential role of sAC in regulating photosynthesis in *T. pseudonana*. To this aim, I will begin by revising key aspects of diatom evolution and photosynthesis, and provide an overview of the functions of sAC in better studied organisms.

Evolution of Marine Diatoms

Diatoms are believed to have originated from a secondary endosymbiotic event whereby a heterotrophic protist engulfed a red alga, but instead of digesting it, the alga was reduced to a secondary plastid (Yoon et al, 2002). A similar origin was proposed for other algal lineages such

as haptophytes, sporozoan, and cryptophytes (reviewed in Stoebe and Maier, 2002; Keeling, 2009). Endosymbiotic events can be an evolutionary source for the origin of new cellular organelles and can result in novel adaptations for the host cell and symbiotic organism (Gentil et al., 2017).

As a result of the secondary endosymbiotic, diatom plastids are surrounded by a double-membraned chloroplastic endoplasmic reticulum (ER) derived from the host cell (Figure 1) the and series of vesicles known as the periplastidal reticulum (Gibbs, 1979). Additionally, the plastids have the typical chloroplast envelope, which is comprised of two membranes (Bedoshvili et al., 2009; Lee and Kugrens, 1998). The thylakoids are found inside the chloroplast envelope, and it is inside the thylakoids where the photosystems and enzymes from the Calvin-Benson cycle are located. But for photosynthesis to occur, carbon dioxide (CO_2) in the tylakoids must achieve a high enough concentration of carbon dioxide (CO_2) to sustain the activity of Ribulose-1,5-bisphosphate carboxylase/oxygenase (Rubisco), the key enzyme for carbon fixation. The transport of dissolved inorganic carbon (DIC) in the form of bicarbonate (HCO_3^-) and CO_2 is mediated by the chloroplastic ER, periplastidal reticulum, and chloroplast envelope, which contain HCO_3^- transporting proteins, carbonic anhydrase (CA) enzymes that catalyze the interconversion between CO_2 and HCO_3^-, and mediate the acidification of the inter-membrane spaces (reviewed in Matsuda et al 2017). Altogether, these processes constitute a carbon concentrating mechanism (CCM) that allows for higher concentrations of CO_2 to be accumulated between the various membranes surrounding the plastid, and eventually at the site of Rubisco. Thus, CCMs are essential for diatom photosynthesis.

Rubisco's low affinity for CO_2

Rubisco is a crucial enzyme in the photosynthesis process of primary producers and is broadly considered as the most rate-limiting protein in the carbon fixation mechanism (Badger et al., 1998). However, Rubisco has a low affinity for CO_2 and, depending on their relative concentrations, can use oxygen (O_2) instead of with CO_2. The use of O_2 by Rubisco is known as photorespiration, and it can be problematic for the cell because it increases metabolic demand, decreases carbon fixation rates, and produces 2-phospho-glycolate which can damage the chloroplasts (Badger & Andrews, 1987; Tcherkez et al., 2006).

The underlying reason for Rubisco's low affinity for CO_2 is that it evolved during a time when the environmental CO_2 levels were much higher than in modern times, and O_2 levels were much lower. Under those conditions, Rubisco was able to fix CO_2 with little possibility of oxygenase activity (Badger & Andrews, 1987). However, the continuous activity of photosynthetic organisms during hundreds of millions of years resulted in a decrease in atmospheric CO_2 levels and a simultaneous increase in atmospheric O_2 levels to modern levels (Falkowski et al. 1998). This lower CO_2/O_2 ratio in the atmosphere imposed an increased need for photosynthetic cells to develop mechanisms to concentrate CO_2 around the site of Rubisco to ensure carbon fixation over photorespiration, the CCMs.

Carbon concentrating mechanisms (CCMs)

As explained above, the modern CO_2 concentration in the atmosphere and aquatic environments is not high enough to support carbon fixation by Rubisco. As a result of this CO_2 limitation, photosynthetic organisms in both the aquatic and terrestrial environments have developed CCMs to concentrate the necessary amounts of CO_2 at the site of Rubisco for carbon

fixation. In addition, the low diffusion rate of CO_2 in water and the slow rate of CO_2 formation from HCO_3^- results in a much higher availability of HCO_3^- compared to CO_2 for aquatic photosynthesizes (Matsuda et al. 2017; Tcherkez et al., 2006). In response, many aquatic photosynthetic organisms have developed CCMs that utilize both CO_2 and HCO_3^-. In the case of diatoms, the CCM must necessarily involve the multiple membranes and inter-membrane spaces found within the cell to move CO_2 and HCO_3^- from the external environment toward the site of Rubisco.

Environmental CO_2 is hypothesized to passively diffuse through the outer plasma membrane and into the cytoplasm. This is enabled by the hydration of CO_2 into HCO_3^- in the cytoplasm that maintains a low CO_2 concentration, and this condition is sustained by the transport of HCO_3^- through the chloroplastic ER, the periplastidal reticulum and the chloroplast envelopes. At the site of Rubisco, HCO_3^- is converted back into CO_2 for immediate use in carbon fixation (Hopkinson, 2014). The reversible hydration of CO_2 into HCO_3^- is catalyzed by the enzyme carbonic anhydrase (CA), while the movement of HCO_3^- across the various membranes is facilitated by HCO_3^--transporting proteins.

Carbonic anhydrases (CAs)

The localization and subtypes of CAs are diverse and vary among diatom species. At least 10 putative CA genes are present in the genome of *P. tricornutum*, and at least 13 putative CA genes are present in the genome of *T. pseudonana* (Tachibana et al., 2011; Samukawa et al., 2014). In *P. tricornutum,* each CA subtype is present in a specific cellular compartment: α-CAs are located in the chloroplast membranes, β-CAs are located in the pyrenoid, γ-CAs are located in the mitochondria, and θ-CAs are located in the thylakoid (Tachibana et al., 2011). Strangely,

no CA isoform has been identified in the cytosol of this diatom species. In *T. pseudonana,* the different CA isoforms may be present in more than one subcellular location and do not necessarily match the localizations established for *P. tricornutum*. Out of the 13 CA genes, an α-CA is present in the stroma, one γ-CAs was found in the cytosol, three other γ-CAs are inside mitochondria, three δ-CAs are each inside mitochondria, in the chloroplast membrane, and external (in the periplasm), and one ζ-CA is external (Tachibana et al., 2001, Samukawa et al., 2014). No β-CAs have been found, and no CA has been identified in the pyrenoid. The external isoforms of CAs identified are located in the periplasm and have been hypothesized to assist with CO_2 and HCO_3^- uptake at the cell surface. (Samukawa et al., 2014). The variation in location of CAs between *P. tricornutum* and *T. pseudonana* suggests diatom species-specific CCMs in which CAs play different roles in the diverse array of strategies for controlling CO_2/ HCO_3^- flow in conjunction with HCO_3^- transporters.

HCO_3^- transporters

A solute carrier (SLC) family of ten putative HCO_3^- transporters has been identified in the genome of *P. tricornutum*. However, only for one of the coded proteins, known as ptSLC4-2, has its subcellular localization been established (Nakajima et al., 2013). The presence of ptSLC4-2 in the plasma membrane indicates a role in the direct uptake of DIC from the seawater. Although two other SLC4s, (ptSLC4-6 and ptSLC4-7) are predicted to be localized within the four layers of chloroplast membranes, their function and intracellular locations have not been experimentally established. At least two SLC4 homolog exists in *T. pseudonana*, tpSLC4-1 and tpSLC4-2 (Nakajima et al., 2013); their subcellular localizations have not been established.

The cyclic adenosine monophosphate (cAMP) pathway

Cyclic adenosine monophosphate (cAMP) is a signaling molecule that can regulate virtually every aspect of cell biology *via* post-translational modifications on target proteins (Cooper, 2003). cAMP is produced by a type of enzymes called "adenylyl cyclases", of which there are many classes. The most widespread is Class III, which are present in both prokaryotes and eukaryotes and contain multiple members (Linder and Schultz, 2003). Regardless of its source, cAMP acts on exchange protein activated by cAMP (EPAC) and protein kinase A (PKA), which in turn activate or deactivate target proteins that contribute to the regulation of cellular functions. For example, PKA can phosphorylate transcription factors, thus modulating gene expression and transporting proteins that determine the movement of ions across membranes (Cooper, 2003), among many other functions. In marine diatoms, there is evidence for the regulation of CCM-related enzymes and genes through the cAMP pathway in response to environmental changes.

Involvement of the cAMP pathway in diatom CCMs

Several studies in *P. tricornutum* indicated that the expression of CCM-related genes is responsive to environmental CO_2 levels. The transcription of ptSLC4-1, ptSLC4-2, and ptSLC4-4 is activated under lower than atmospheric CO_2 conditions (low CO_2 levels), and repressed in 5% CO_2 (high CO_2 levels) (Nakajima et al., 2013). In addition, the transcriptions of two β-CA genes, ptca1 and ptca2, are downregulated under high CO_2 levels (Harada et al., 2006). This study also showed an increase in cAMP levels under elevated CO_2, and a repression of gene expression in diatoms exposed to ambient CO_2 levels but treated with two agonists of the cAMP pathway (Harada et al., 2006). In *T. pseudonana*, a more environmentally relevant elevated CO_2

level of 0.08% (or 800 µatm) was shown to regulate the expression of several putative CCM- and photorespiration-related gene clusters (Hennon et al., 2015). Subsequently, they established that the downregulation in δ-CA3 gene expression depended on cAMP, but that of *pID 262258* (a putative Na^+/H^+ transporter) did not. In summary, the combined evidence indicate that the cAMP pathway plays an essential role in the regulation of CCM-related genes in response to elevated CO_2 in diatoms. However, the source(s) of cAMP are not known.

Soluble adenylyl cyclase (sAC)

The soluble adenylyl cyclase (sAC) is a cAMP-producing enzyme that is directly stimulated by HCO_3^-, and therefore is a good candidate for regulating the CCM of marine diatoms. Although sAC was discovered in mammals, it was recognized that its two catalytic domains were closely related to adenylyl cyclases from cyanobacteria (Buck et al 1999). Subsequently, the cAMP producing activities of sAC and sAC-related enzymes were found to be directly activated by HCO_3^- in mammals (Chen et al., 2000; Litvin et al, 2003; Kleinboelting et al. 2014), cyanobacteria (Chen et al., 2000; Cann et al, 2003), chloroflexi bacteria (Kobayashi et al, 2004) and fishes (Tresguerres et al 2010, Salmeron et al 2021). Since its discovery ~20 years ago, sAC has been reported to act as a key acid/base sensing enzyme that regulates multiple physiological processes in mammals (reviewed in Tresguerres et al, 2011) as well as in diverse aquatic organisms (reviewed in Tresguerres et al., 2014; also see Barott et al. 2017, 2020; Lo et al. 2020; Roa and Tresguerres 2016).

In diatoms, sAC-like genes have been identified in *P. tricornutum* and *T. pseudonana* (Matsuda et al., 2011). In the latter, the proteins coded by Thaps3-24827 and Thaps3-22442 share many key structural similarities with the human sAC protein, which is well characterized

(Steegborn, 2014; Kleinboelting et al., 2014). These include the presence of two catalytic domains C1 and C2 (Figure 2) containing the amino acids essential for binding to ATP, catalytic metals, and HCO_3^- (Figure 3). Furthermore, HCO_3^--stimulated cAMP production was reported in lysates from both species (Matsuda et al., 2011; Tresguerres, 2014). However, the physiological roles of these diatom sAC-like enzymes remain unknown.

Interestingly, sAC from animals undergo extensive alternative splicing, resulting in multiple isoforms, and some of these isoforms can be preferentially located in specific subcellular compartments such as the cytosol, the nucleus, and mitochondria (Zippin et al, 2002, 2004; Valsecchi et al. 2014). In addition, animals possess additional sources of cAMP known as "transmembrane adenylyl cyclases" (tmACs), which as their name indicates, are embedded in the cell membrane. Thus, cAMP is generated independently in microdomains throughout the cell that can regulate independently specific targeted mechanisms (reviewed in Tresguerres et al., 2011, 2014; Zippin et al, 2002). This suggests that various ACs play roles in the regulation of multiple different cellular mechanisms. In green algae, it has been shown that an AC and cAMP pathway participate in blue light responses (Iseki et al, 2002) and cell division (Carré and Edmunds, 1993), though the roles of sAC in marine diatoms have not been confirmed.

The specific sAC inhibitor KH7

Elucidating the physiological role(s) of a given protein requires the ability to specifically modulate its activity and detect its effect on a process(es). The small molecule (E)-2-(1H-Benzo[d]imidazol-2-ylthio)-N′-(5-bromo-2-hydroxybenzylidene) propanehydrazide, known as KH7, specifically inhibits sAC from animals with a half maximum inhibitory concentration (IC_{50}) of ~10μM (Bitterman et al., 2013, Hess et al., 2005, Tresguerres et al 2010). In

mammalian cells, high KH7 concentrations of 50 μM may induce non-specific effects on mitochondrial function and ATP production through mitochondrial uncoupling (Jakobsen et al., 2018). However, these effects were ruled out in coral cells. (Barott et al., 2017), and toxic side-effects were also absent in fish (Lo et al., 2020). Moreover, KH7 concentrations of up to 1 mM do not significantly inhibit the activity of tmACs (Roa and Tresguerres 2016), making KH7 an excellent reagent to study the physiological roles of sAC. Importantly, KH7 has been shown to inhibit the HCO_3^--stimulated fraction of cAMP production in *T. pseudonana* lysates (Tresguerres, 2014), which establishes KH7 as a viable reagent to study sAC's physiological roles in marine diatoms.

Thesis Goals

This thesis aimed to confirm the presence of sAC in the marine diatom *T. pseudonana*, and gain some understanding of its possible role in the CCM and photosynthetic mechanism. Initial efforts were made to establish the subcellular localization of two sAC proteins by creating transgenic diatom cells expressing sACs tagged with enhanced green fluorescent protein (eGFP). sAC localization was hypothesized to be found within the cell cytoplasm, where together with CAs could help regulate the uptake of CO_2 and HCO_3^- from the external environment. In addition, sACs could be inside mitochondria or chloroplasts and regulate the electron transport chains associated with respiration and photosynthesis, respectively. Moreover, sACs could be present in the nucleus and regulate gene expression through the PKA-dependent phosphorylation of transcription factors. Unfortunately, this part of the thesis could not be completed, in part because the large size of the two sAC genes greatly complicated cloning efforts, and in part because COVID-19 disrupted all research activities during March-December 2020. Thus, an

alternative plan was formulated to assess the potential role of sAC in modulating diatom photosynthesis by testing the effect of KH7 on photosynthetic O_2 production.

Methods

T. pseudonana stock cultures

T. pseudonana (CCMP1335) cultures were grown axenically in artificial seawater (ASW) (Darley & Volcani, 1969) only for the "KH7 wash out experiments". Cultures were grown in ASW supplemented with half-strength Guillard's "f" solution (F/2 medium) (Guillard and Ryther, 1962) for the rest of the experiments. Cloning experiments were performed on wild type *T. pseudonana*, while all O_2 evolution experiments were conducted on a transgenic *T. pseudonana* line that constitutively expresses the V-type ATPase B subunit fused to enhanced fluorescent protein (*T. pseudonana* VHA_B-eGFP) (Yee et al., 2019). Cultures were grown under continuous illumination at 70 μE at 18°C.

Cloning and generation of sAC-eGFP conjugation plasmid

The genes of interest Thaps3 -24827 and Thaps3-22442 were cloned using genomic DNA (gDNA) isolated from wild type *T. pseudonana,* the Phusion High-Fidelity PCR Master Mix (New England Biolabs) and custom primers (Table 1). Invitrogen Gateway cloning was originally used to form a sAC-eGFP expression plasmid. This method is a two-reaction that utilizes a gateway entry vector (pENTR) to clone PCR product that do not contain *att* sites, and a destination vector that recombines with the entry vector during an LR reaction to form the expression clone. Later, a plasmid containing the fcp promoter, eGFP and fcp terminator sequences (Karas et al., 2015) provided the backbone to build the final fcp-sAC-eGFP conjugation plasmid for use in Gibson cloning (generously provided by the Andrew Allen Lab, JCVI). However, this plasmid also contained the gene TpSil3p and it was necessary to remove it before inserting the genes of interest. To make this plasmid usable for the cloning processes, the restriction enzyme NcoI (New England Biolabs) was used to cut open the plasmid. Once the

plasmid was linearized, primers were designed to isolate and amplify the desired pieces of the backbone while omitting the TpSil3p gene; the goal was to combine the backbone with the genes of interests through Gibson cloning.

Cultures for O_2 measurements

T. pseudonana VHA-eGFP were grown in 50 ml of F/2 media to a density of ~2-3 x 10^6 cells/ml. They were then used to inoculate 1L elongated tubes to a starting density of ~1 x 10^5 cells/ml within a specialized culturing system (generously loaned by Dr. Greg Mitchell, SIO) that kept temperature at 18˚C using a water-jacketed container. The culture tubes were exposed to continuous illumination of ~50 µE. Each tube was bubbled with filtered air, which contained ~500 parts per million (ppm) CO_2. Cultures were allowed to grow continuously for two days before conducting the O_2 measurements. Cell density measurements were taken using a hemocytometer. A pH sensor (Denver Instrument) and Corning 965 Carbon Dioxide Analyzer were used to collect pH and total CO_2 measurements for all cultures except the culture used for the washout experiment (Table 2).

KH7 incubation

Samples from a single culture (*n*=1) (October 20-22, 2020) grown under the experimental conditions described previously were used to create a KH7 dose-response curve of KH7 on O_2 production rates. Culture aliquots (2 mL at ~925,000 cell/ml) were placed in an 18°C water bath and maintained in the dark until testing. A 30 mM KH7 (Tocris Bioscience; ≥ 98% purity) stock solution prepared in dimethyl sulfoxide (DMSO), and appropriate volumes were added to various culture aliquots to achieve a final KH7 concentration of 10 µM, 5 µM, 4 µM, 3 µM, and 2 µM. The 10 µM KH7 dose was applied to two different culture aliquots. The KH7-treated

culture aliquots were incubated for ~45 minutes before O_2 measurements were taken. Previous results in the Tresguerres laboratory indicate that equivalent volumes of DMSO do not significantly affect O_2 production rates in *T. pseudonana.* Because of this, DMSO was not added to control aliquots for any of the trials (Daniel Yee, personal communication).

At a later date (November 12-14, 2020), the effects of 10 and 20 μM KH7 were tested on three additional cultures (*n*=3). Since the three cultures had different cell densities, they were centrifuged at 4500 RCF for 10 minutes and the diatom-containing pellets were resuspended in F/2 media to achieve a density of ~ $1x10^6$ cell/ml, and treated as described above. However, in this case the 2 mL culture aliquots were dosed with 10 μM KH7, 20 μM KH7, or left untreated as controls.

The reversibility of the effects of KH7 inhibition on photosynthetic O_2 production were investigated by "washing out" the inhibitor by incubation in fresh medium. To this aim, one culture (*n*=1) (August, 27, 2020) was grown in a 50 ml flask at 18°C in ASW (without f/2 supplements) under constant illumination at ~50 μE on a shaker plate. The culture was grown to a cell density of ~$4x10^6$ cells/ml. Two 10 mL culture aliquots were placed in a dark, 18°C water bath; one aliquot was dosed to a final concentration of 10 μM KH7 and the other was not treated to act as the control. After taking O_2 measurements in both culture aliquots, cells were centrifuged down at 4500 RCF for 10 minutes, the medium was carefully removed, and resuspended in fresh ASW containing DMSO. Culture aliquots were incubated in a rotator for 10 minutes This "wash out" process was performed three times. The washed-out cultures were then placed back into the dark, 18°C water bath for at least 10 minutes before taking O_2 measurements for a second time.

O_2 Measurements

A Hansetech Oxy-lab oxygen electrode was used to measure photosynthetic O_2 production by diatom cultures. The temperature within the chamber was maintained at 18°C. Samples (2 mL) were loaded into the machine and exposed to ~1300 µE of light for a 10-minute interval to measure net O_2 production (NOP) (µmol/ml/min). Oxygen consumption (OC) (µmol/ml/min) was measured during a ~2-minute period post light exposure. Rates were calculated using the slope of measurements during each of these time periods. Gross O_2 production (GOP) rate was calculated following the equation:

$$GOP = NOP - OC$$

GOP was then normalized by cell numbers to end with a rate of O_2 production (fmol/cell/min). O_2 percent decrease was calculated as:

$$(GOP\ KH7 / GOP\ Control) * 100$$

Confocal Imaging

Super-resolution confocal microscopy was used to image *T. pseudonana* VHA_B-eGFP untreated control cells or with KH7 at a final concentration of either 10 µM or 20 µM. The cells were also incubated with MitoTracker™ Orange CMTMRos (ThermoFisher Scientific) at a final concentration of 0.1µM to stain mitochondria. Cells were spun down and washed one time with fresh F/2 before being transferred to a 35 mm poly-d-lysine coated glass bottom petri dish and mounted on a Warner Instruments QE-1HC Quick Exchange Heated/Cooled stage chamber controlled by CL-200 Dual Channel Temperature Controller which was maintained at 18 °C. Cells were imaged with a Zeiss LSM800 inverted confocal microscope equipped with a Zeiss Plan-Apochromat 63× (1.4) Oil DIC M27 objective, and Zeiss Airyscan super-resolution

detector. Four channels were acquired to monitor eGFP (Ex 488 nm with 0.3% laser power, Em 509 nm, detection 490-535 nm), MitoTracker fluorescence (Ex 554 nm with 0.2% laser power, Em 576nm, detection 490-607 nm) and Chl autofluorescence (Ex 655 nm with 0.2% laser power, Em 667, detection 450-700).

Data Analysis

The effects of KH7 on GOP rates, NOP rates and OC rates for the main experimental trial were analyzed using a one-way ANOVA test. The level of statistical significance was set at $p < 0.05$. Multiple comparisons were conducted using post-hoc Dunnett's multiple comparison test. Standard error mean was also calculated. Data analysis was completed using GraphPad Prism v.9.

Results

Cloning of Thaps-22442 and Thaps-24827 and attempts to creating eGFP-fusion constructs

Custom primers (Table 1) were designed to clone the sAC-like genes Thaps-22442 and Thaps-24827 from *T. pseudonana* gDNA, and their annealing PCR temperatures were initially calculated using the online New England Biolabs (NEB) Tm calculator. After extensive troubleshooting of annealing temperatures and primer sets, PCR products of ~5.6 kilobase pairs (kpb) and ~6.8 kpb were obtained, which respectively match the predicted sizes for Thaps3-22442 and Thaps3-24827 (Figure 4). The identities of the PCR products have not been confirmed through sequencing due to disruptions from COVID-19 and difficulties purifying the product in high enough concentrations. In addition, multiple attempts to create Thaps-22442 and Thaps-24827 eGFP-fusion constructs using the Invitrogen Gateway cloning failed during the BP recombination reaction that creates the entry vector, despite increasing the concentration of PCR product and donor vector used. Next, the two-piece Gibson cloning method was attempted using the plasmid pTpPuc3 as a backbone that contains the fcp promoter and terminator and the eGFP sequence. However, pTpPuc3 contained another gene TpSil3p, which needed to be removed before inserting Thaps-22442 and Thaps-24827. Unfortunately, multiple attempts that included testing various annealing temperatures, designing and using additional primer sets, and a three-piece Gibson assembly method were unsuccessful. Furthermore, these additional efforts to generate Thaps-22442 and Thaps-24827 eGFP-fusion constructs were curtailed due to COVID-19 restrictions to research. Thus, this prevented the generation of transgenic *T. pseudonana* cell lines expressing fluorescently tagged sAC-like proteins to establish their subcellular localizations.

Effects of sAC inhibition on photosynthetic O_2 production rate

In a preliminary experiment, control *T. pseudonana* cultures exhibited a GOP rate of 15.676 fmol/cell/min. This GOP was inhibited by KH7 in a dose response manner, ranging from a ~30% inhibition with 2μM to a ~93% inhibition with 10μM. (Figure 5). A measurement on an additional culture confirmed the high degree of inhibition by 10μM KH7, which induced a ~90 % decrease in GOP (Figure 7a).

To test whether the effect of KH7 was due to a lethal effect on cells, a "washout" experiment was conducted on aliquots from a different set of cultures (Figure 6). In this second preliminary trial, GOP rate in control cultures was 2.941 fmol/cell/min, which was considerably lower than in the first preliminary trial. While the exact reasons are unknown, it is worth pointing out that the first trial used F/2 medium, but this second trial used ASW. In addition, 10μM KH7 only induced a 52% decrease in GOP (down to 1.412 fmol/cell/min). Washing out the cells in fresh ASW induced an increase in GOP rate in both control (up to 4.471 fmol/cell/min) and KH7-treated (up to 2.824 fmol/cell/min) cells. Furthermore, the difference in GOP rates between cultures was reduced to 36.8%.

To further characterize the effect of sAC inhibition by KH7, a main experimental trial was conducted, this time in triplicate (n=3) and using F/2 medium like in the first preliminary trial. The one-way ANOVA test showed that the differences between the GOP rates were not statistically significantly ($p = 0.1032$), however, there were noticeable differences between the control rates and the rates from the samples treated with KH7. Although the GOP rate of control cultures was similar to that in the first trial (13.499 ± 0.827 fmol/cell/min), the degree of

inhibition by 10μM KH7 was similar to the second trial (down to 6.406 ± 0.509 fmol/cell/min, or a 52.5% ± 2.94% decrease in GOP). To test a potential loss of potency on the KH7 stocks, additional cultures were dosed with 20μM KH7. But despite doubling the concentration of KH7, the inhibition of photosynthetic O_2 production rate remained virtually unchanged at 51.2% (Figure 7b).

Effects of sAC inhibition on O_2 consumption and net O_2 production rates

Since GOP is calculated by subtracting OC rate from the NOP rate, the inhibitory effects of KH7 on GOP could be due to a decrease in NOP, an increase in OC, or a combination. Thus, the effects of KH7 on NOP and OC rates during the third trial were analyzed. The OC rate is taken during the dark period of the O_2 measurements is a proxy for the rate of aerobic respiration. The one-way ANOVA test showed that the differences between the OC rates were not statistically significantly ($p = 0.1687$), however, there was a noticeable increase between the control rate and the 20 μM KH7 rate. The OC rate of control cultures was 3.21 ± 0.197 fmol/cell/min and it was not notably affected by 10μM KH7, which induced a marginal decrease down to 3.072 ± 0.738 fmol/cell/min Increasing the concentration of KH7 to 20 μM did increase the OC rate to 7.222 ± 2.602 fmol/cell/min, or an induced a 135% increase (Figure 8b).

The NOP rate is taken during the light period of the O_2 measurements when O_2 consumption and photosynthetic O_2 production are happening concurrently. The one-way ANOVA test showed that the differences between the OC rates are statistically significant ($p= 0.0007$). Additionally, the Dunnett's multiple comparison test showed that the control rates were significantly different from the rates measured for the samples dosed with 10 μM and 20 μM KH7. The NOP rate of control cultures was 10.290 ± 0.940 fmol/cell/min which was significantly decreased by 10 μM KH7 to 3.334 ± 0.869 fmol/cell/min (adjusted $p = 0.0029$).

This corresponds to a 67.6% ± 5.424% decrease in NOP. Doubling the concentration of KH7 significantly decreased the NOP rate to -0.637 ± 0.320 fmol/cell/min. (adjusted p = 0.0005). This corresponds with a 106% ± 3.109% decrease. (Figure 8a). Altogether, this indicates that 10 μM KH7 predominantly affects processes involved in photosynthetic O_2 production, while 10 μM KH7 additionally increases aerobic respiration rate.

Analyses of the O_2 traces revealed additional interesting information. The O_2 traces from control samples displayed consistent, gradually increasing slopes. (Figure 9). The O_2 traces from cells treated with 10 μM KH7 had less pronounced slopes, as well as some irregularities ("ups" and "downs") that were more evident in some cultures than in others (Figure 10b, c). Finally, the O_2 traces from cells treated with 20 μM KH7 displayed much larger irregularities through both the light exposure and the dark periods: there were multiple sudden and large "ups" and "downs in the O_2 traces for all three culture samples, and very high OC rates during the dark periods in two of the samples (Figure 11b,c). Surprisingly, the third sample seemed to produce some O_2 in the dark (Figure 11a), but the significance if this observation is unclear.

Effects of sAC inhibition on general cell morphology and VHA localization

The increased OC rate and the abnormalities in the O_2 traces induced by 10μM and 20μM KH7 prompted the examination of diatom cell morphology. To this aim, control and KH7-treated cells were imaged using super-resolution confocal microscopy to qualitatively assess potential effects on the size and shape of the plastids (identified based on their chlorophyll signal), and on the location, shape and size of mitochondria (identified using the mitochondrion-specific fluorescent dye, MitoTracker) (Figure 12). In addition, potential changes in VHA localization were examined based on its eGFP tag present in *T. pseudonana* transgenic cell line.

This preliminary survey did not identify any obvious differences in any parameter between the KH7 treated cells and the con

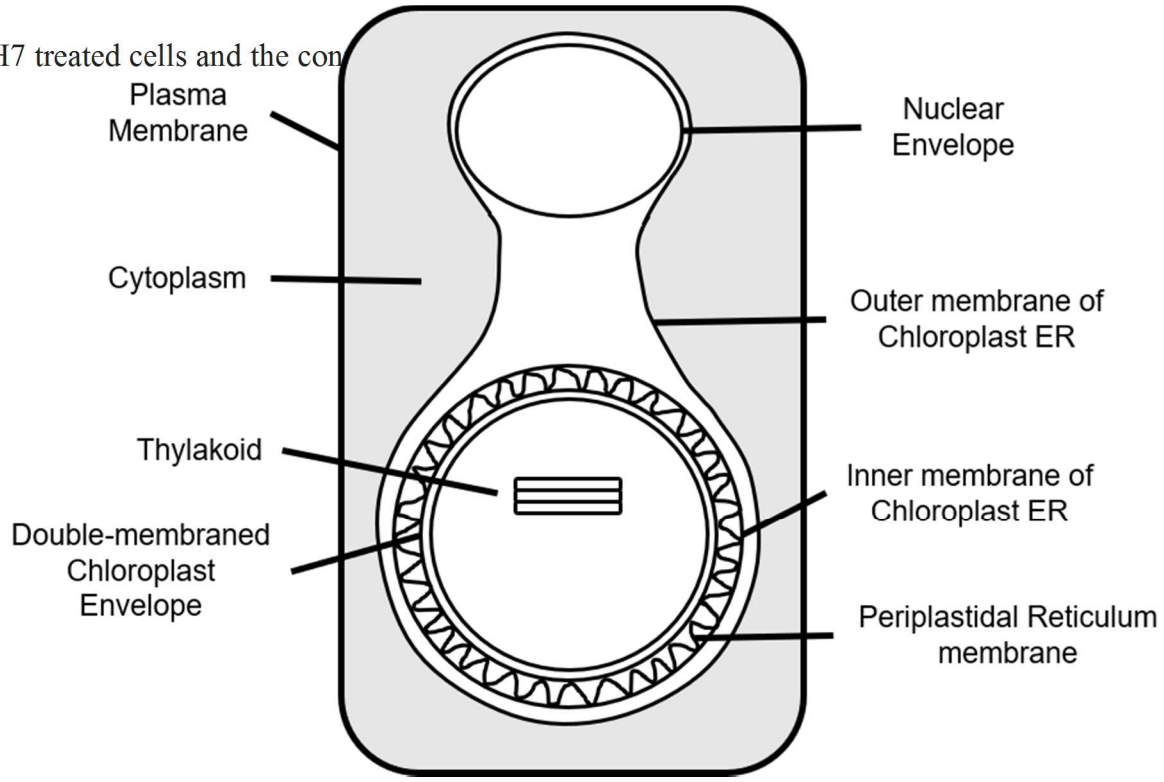

Figure 1: Diagrammatic representation of the various membrane systems and subcellular compartments present in diatoms. Modified from Lee and Krugens (1998).

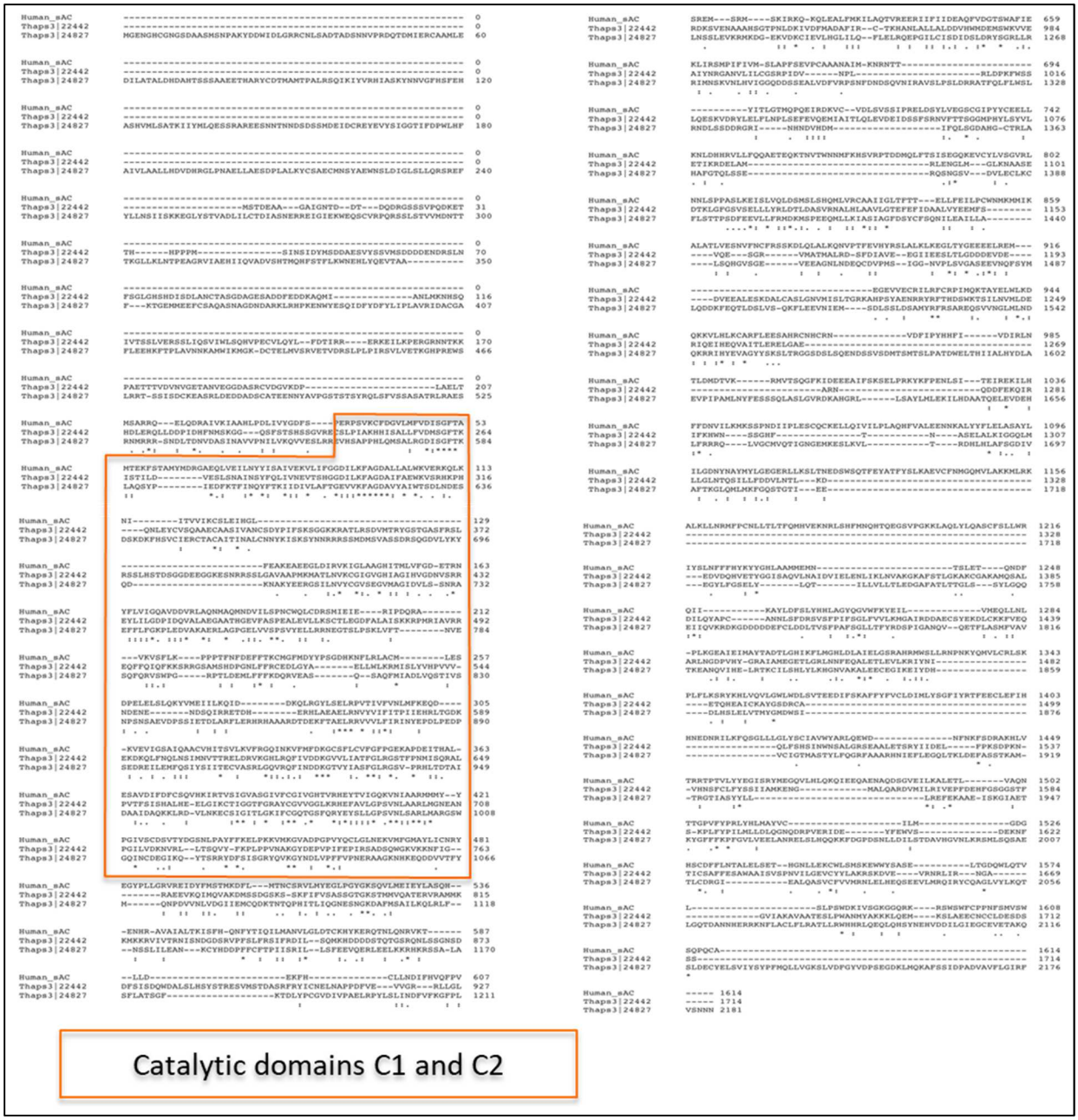

Figure 2: Comparison of the human soluble adenylyl cyclase (sAC) gene and the two putative sAC-like genes in *Thalassiosira pseudonana*, Thaps3-22442 and Thaps3-24827. The two catalytic domains C1 and C2 are boxed in orange.

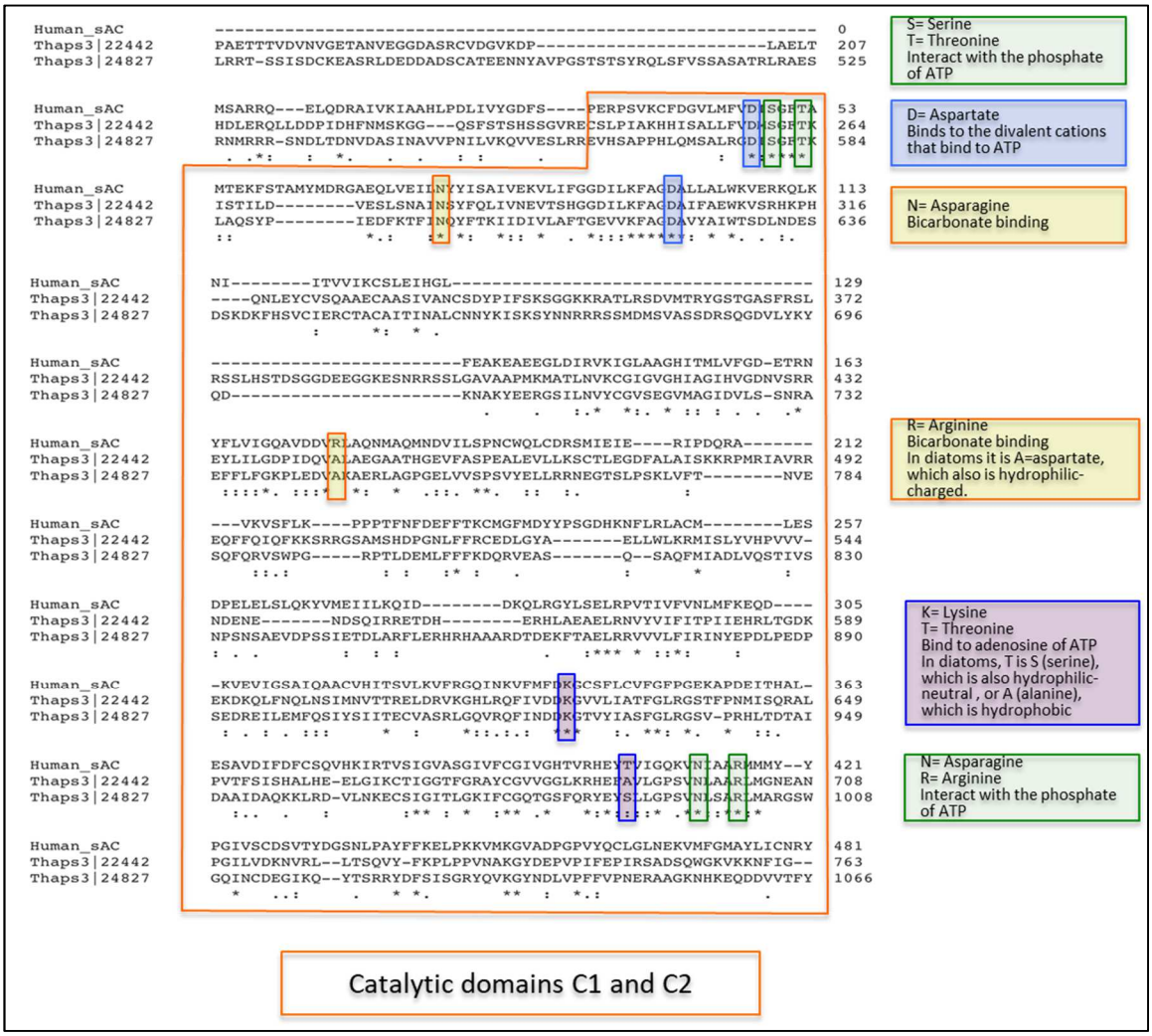

Figure 3: Catalytic domains C1 and C2 for human soluble adenylyl cyclase (sAC) and the two putative sAC-like genes in *Thalassiosira pseudonana* Thaps3-22442 and Thaps3-24827. Conserved amino acids are highlighted with the corresponding-colored box and description of function.

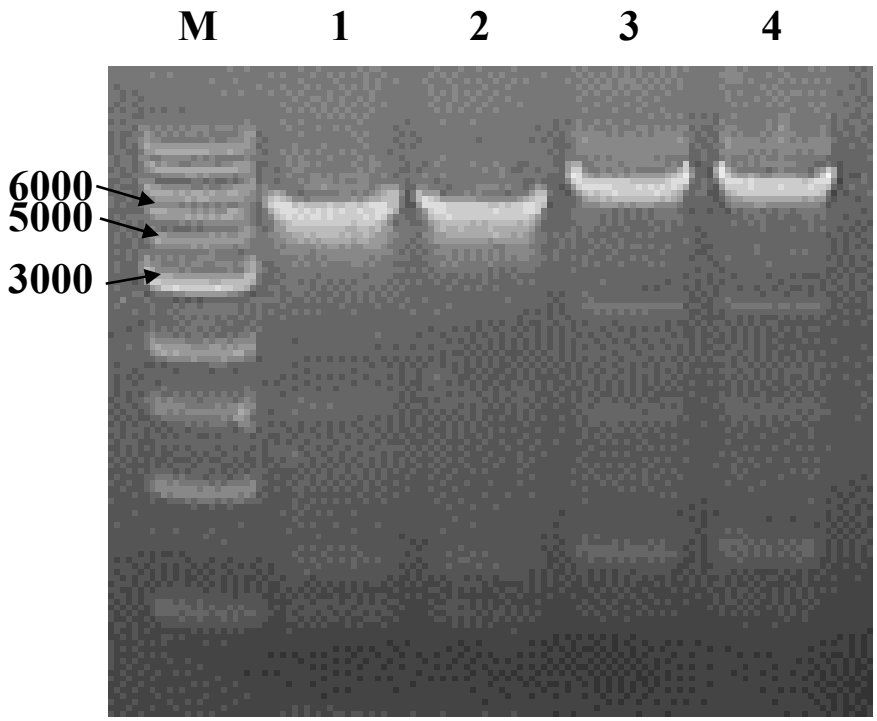

Figure 4: Gel electrophoresis for two putative sAC genes in *Thalassiosira pseudonana.* M: 10 kilobase pair DNA ladder; Lane 1-2: Thaps3-22442; Lane 3-4: Thaps3-24827

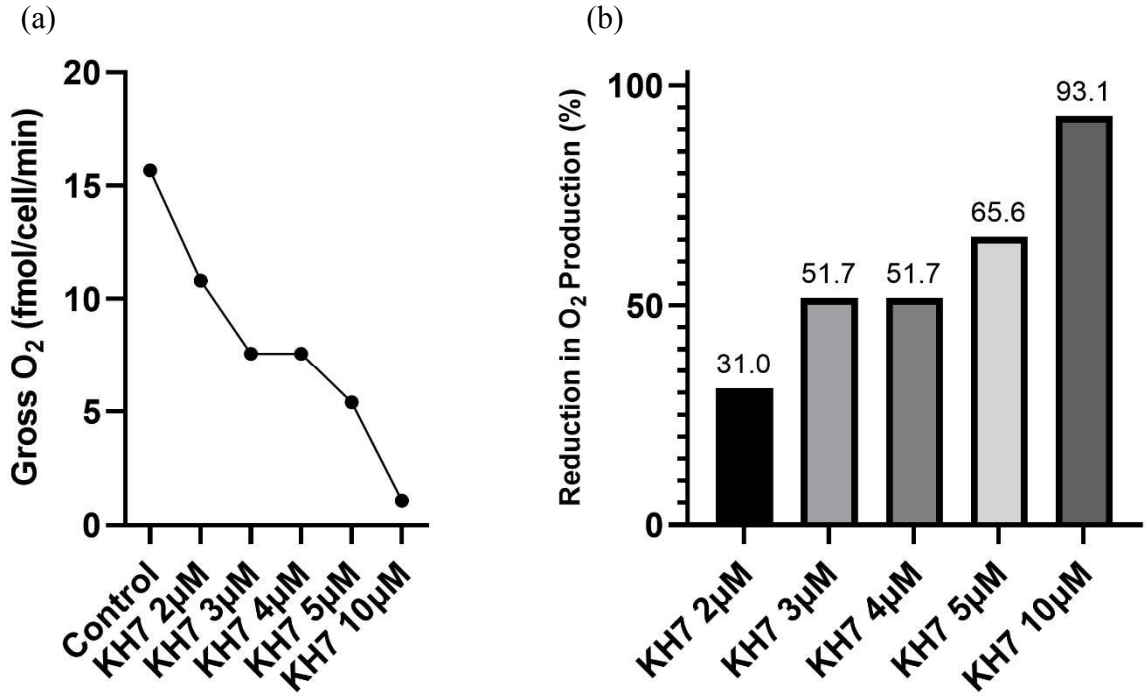

Figure 5: KH7 inhibition dose response results in decreased O_2 production rates as concentration increases. (a) Gross O_2 rates (n=1) for treatments of varying KH7 concentrations. (b) Percent (%) reduction in O_2 production when compared to the control for treatments of varying KH7 concentrations

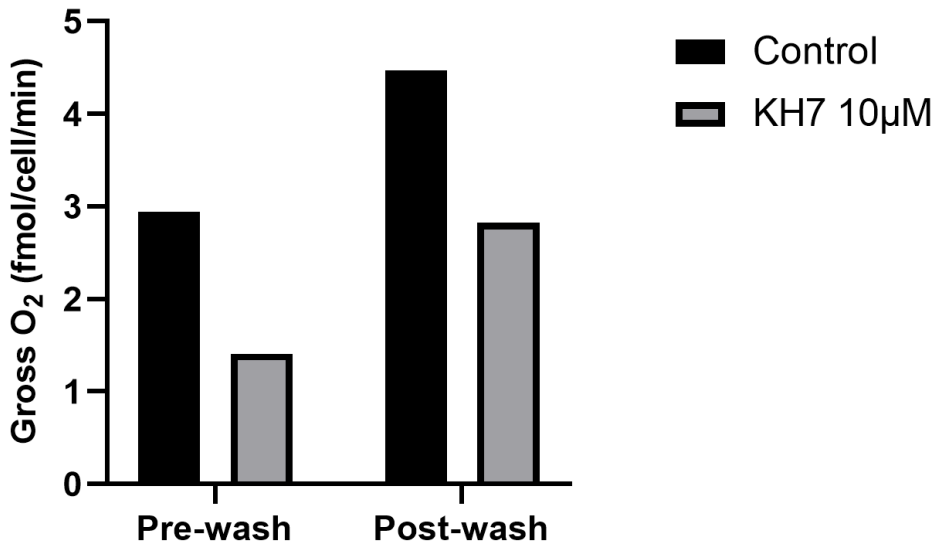

Figure 6: KH7 inhibition effect on O_2 production rates with recovery following washout of the inhibitor. Gross O_2 rates for control and 10μM KH7 treated samples before and after a three-round repetition of washing with fresh ASW media + DMSO. (*n=1)*

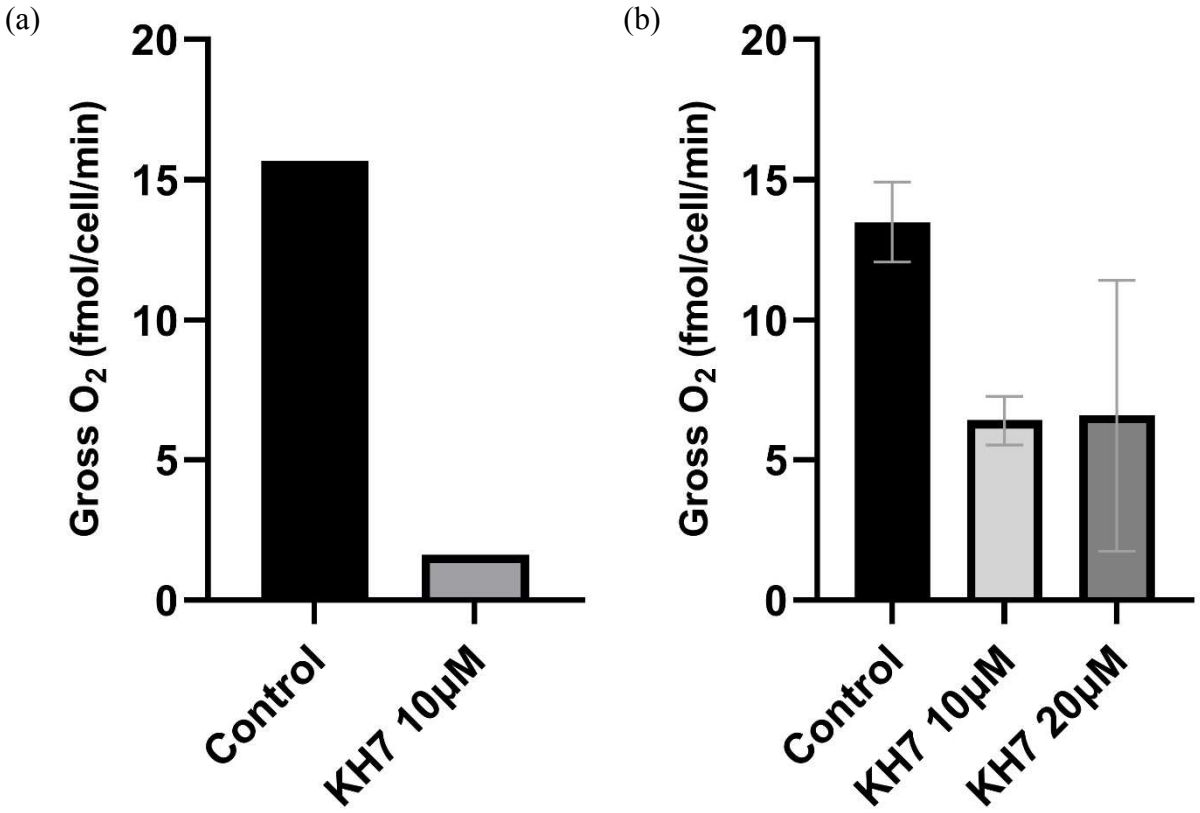

Figure 7: KH7 inhibition results in decreased O_2 production rates at 10μM and 20μM concentrations of KH7. (a) Gross O_2 rates from the first preliminary trial, testing KH7 inhibition (n=1) b) Gross O_2 rates from the third trial testing KH7 inhibition (n=3, error bars = ± standard error mean).

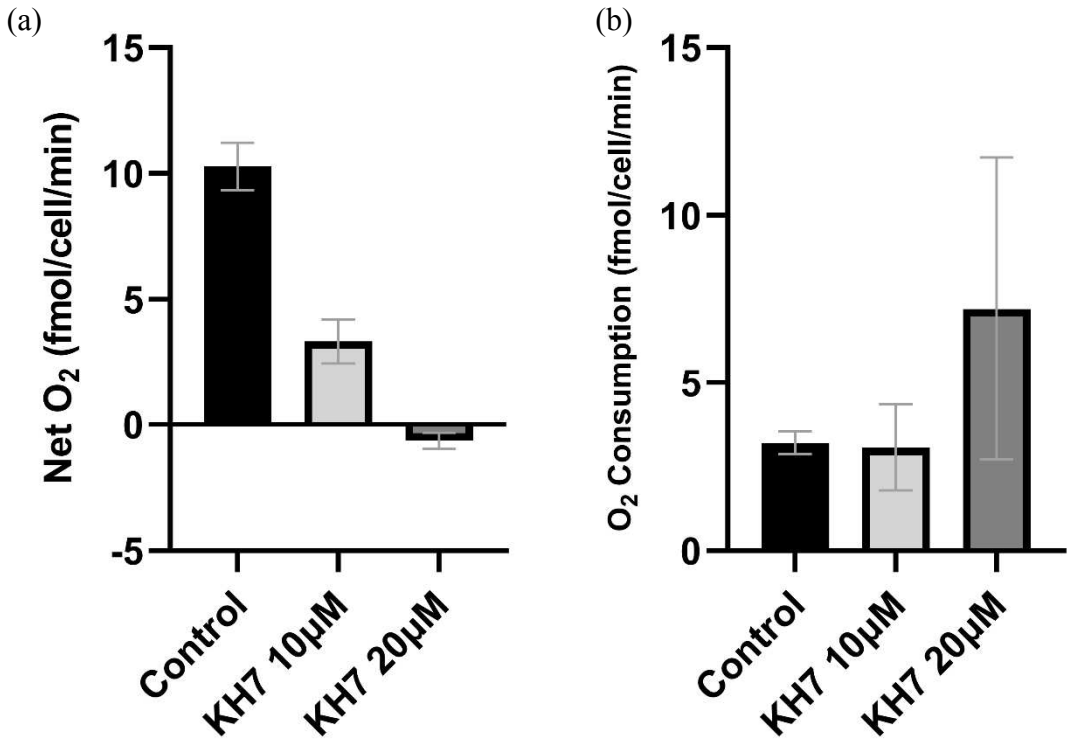

Figure 8: KH7 inhibition effect on a) Net O_2 rates and b) O_2 consumption rates for samples measured during the third trial (*n*=3, error bars = ±Standard Error Mean) testing KH7 inhibition on photosynthetic O_2 production.

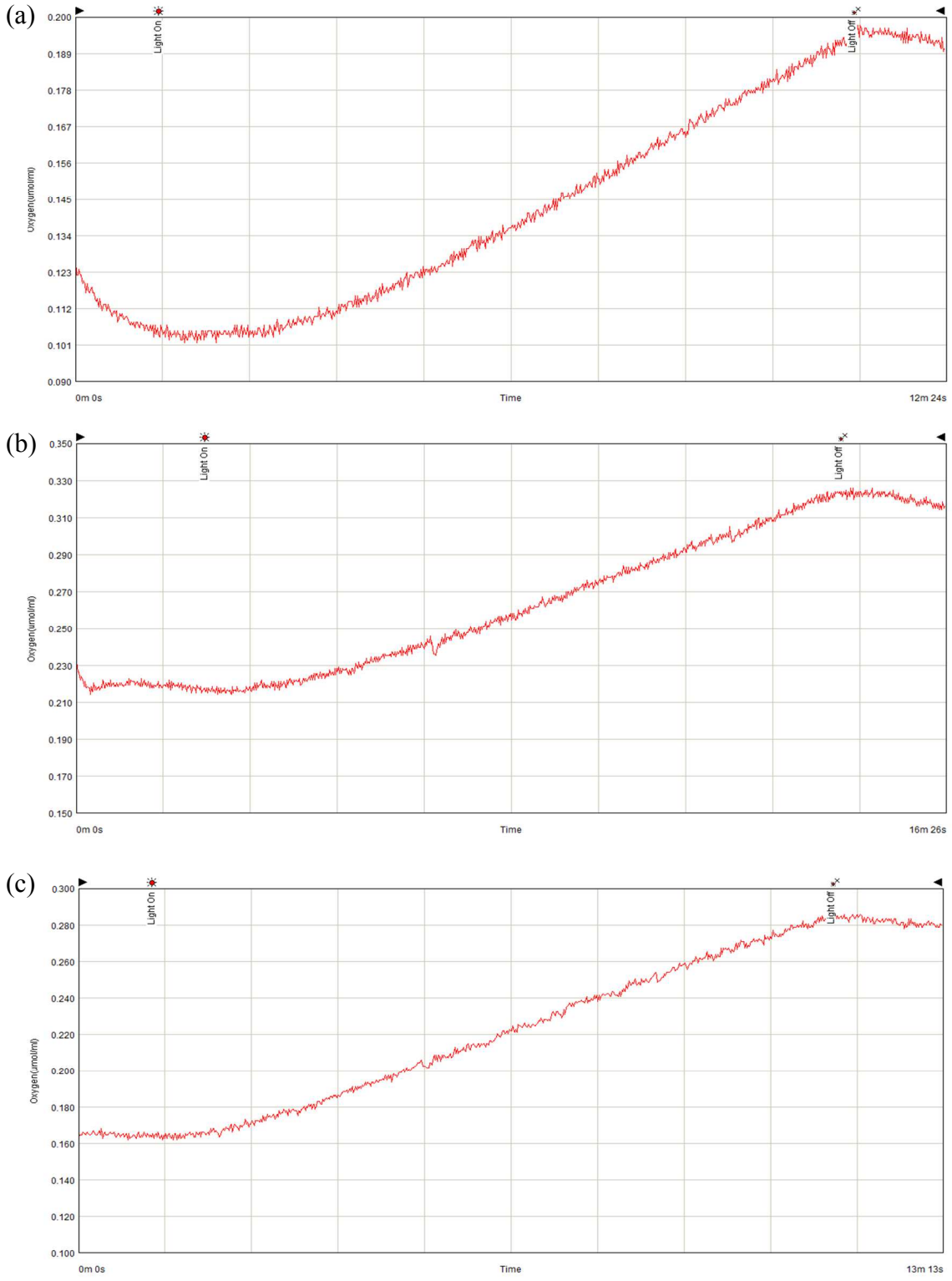

Figure 9: O_2 measurement trace graphs for the three control samples measured during the third trial testing KH7 inhibition on photosynthetic O_2 production. (a) Replicate 1 (b) Replicate 2 (c) Replicate 3.

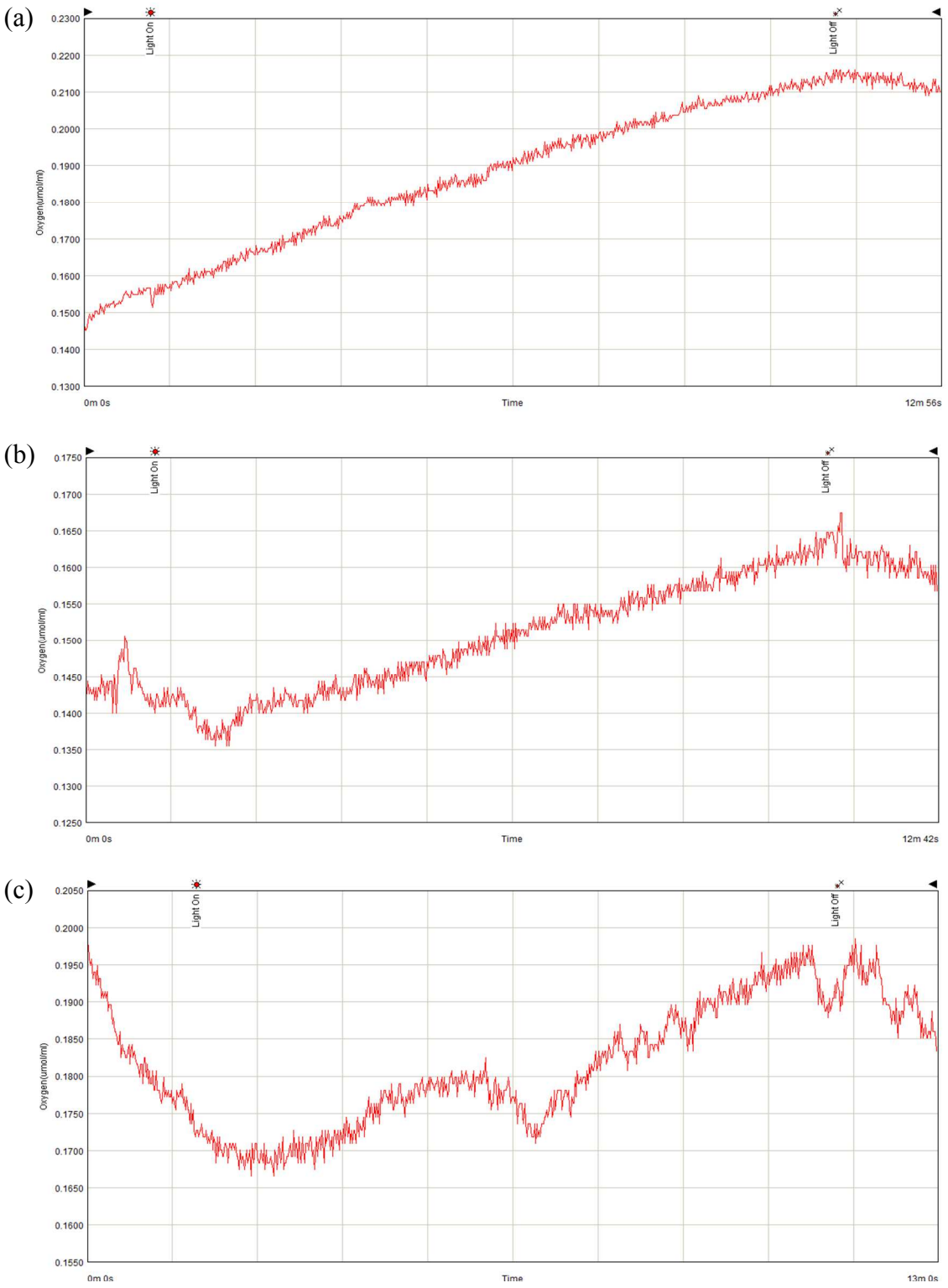

Figure 10: O_2 measurement trace graphs for samples treated with 10µM KH7 measured during the third trial testing KH7 inhibition on photosynthetic O_2 production. (a) Replicate 1 (b) Replicate 2 (c) Replicate 3.

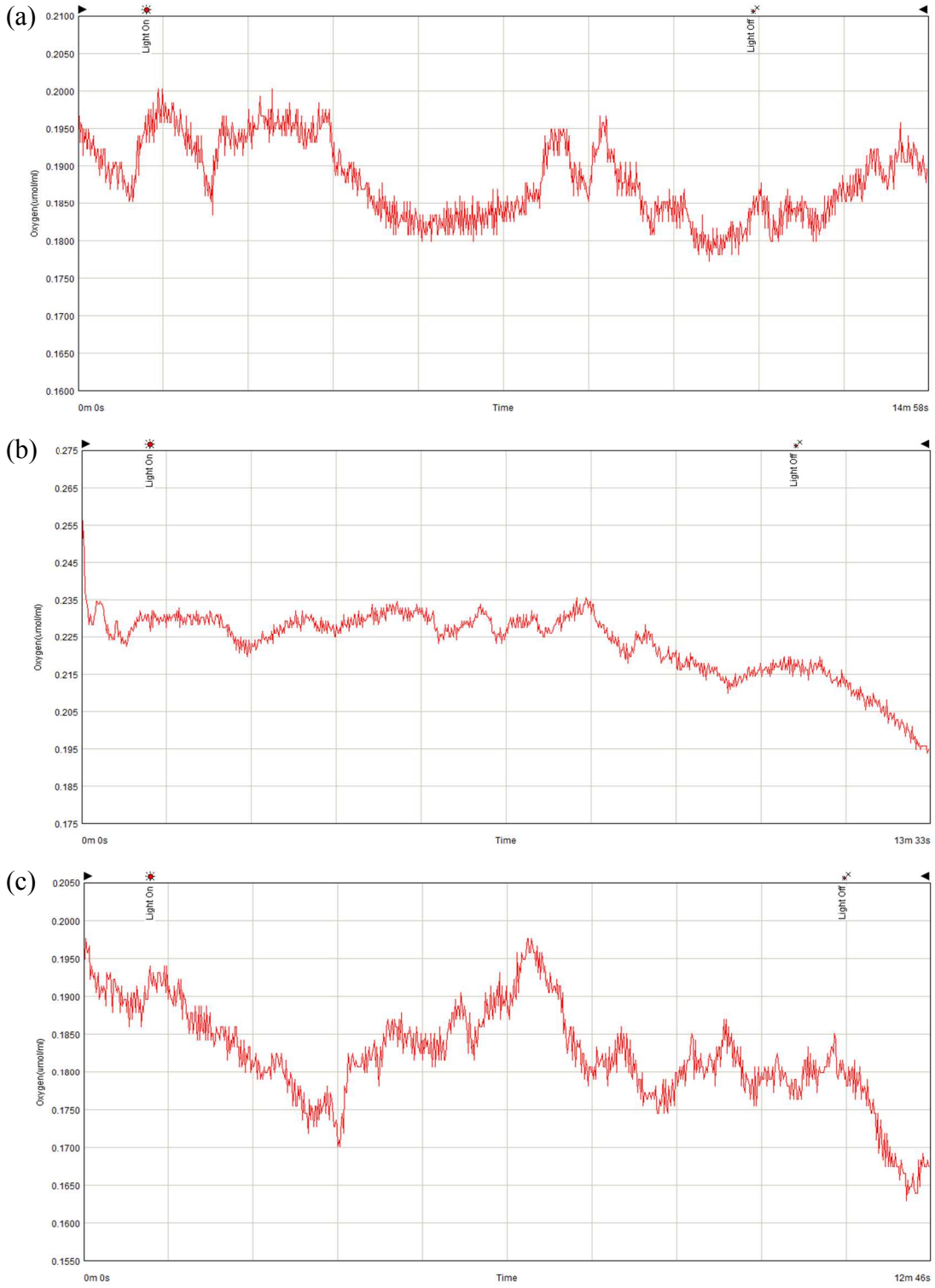

Figure 11: O_2 measurement trace graphs for the samples treated with 20uM KH7 measured during the third trial testing KH7 inhibition on photosynthetic O_2 production. (a) Replicate 1 (b) Replicate 2 (c) Replicate 3.

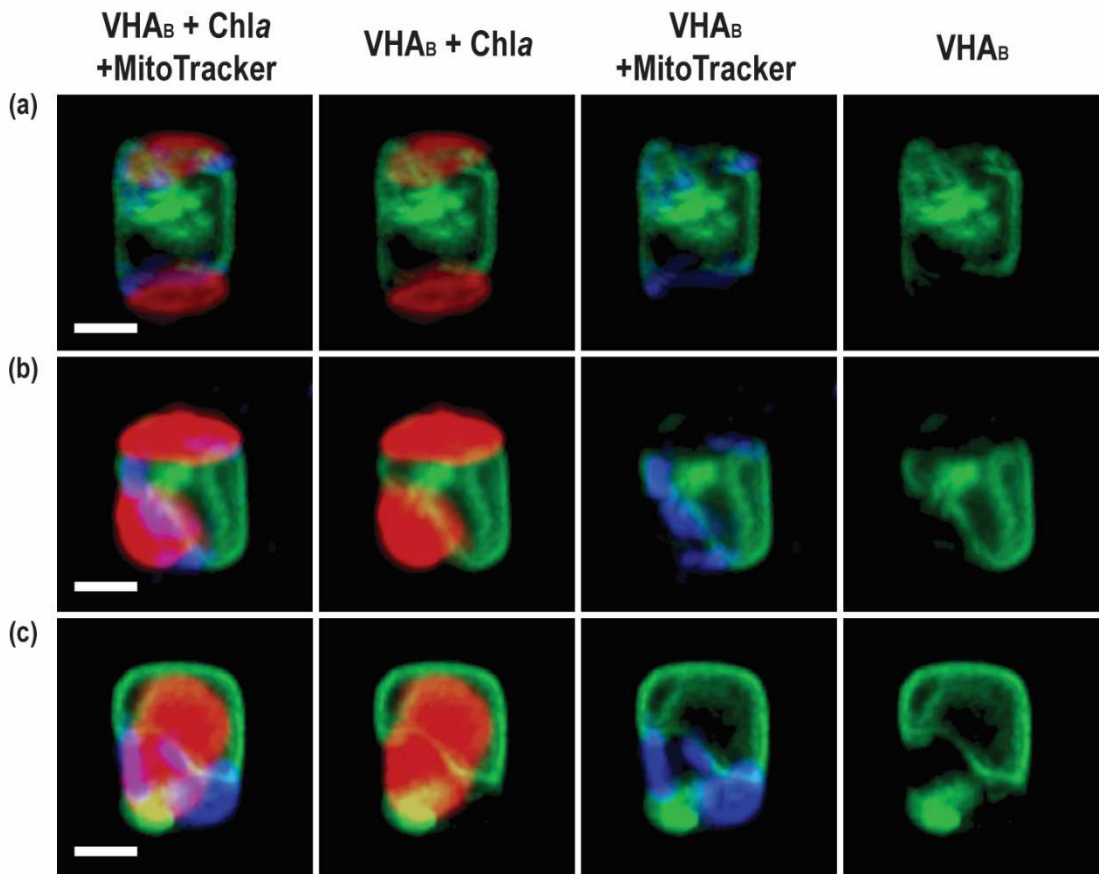

Figure 12: Physiological structures and localization of V-type H^+ -ATPase (VHA) in diatom cells show no obvious differences, under three different treatment conditions. Representative images of exponentially growing *Thalassiosira pseudonana* expressing fcp-VHA_B subunit tagged with enhanced green fluorescent protein in: (a) control (b) treated with 10µM KH7 (c) treated with 20µM KH7. Green, VHABeGFP; red, Chl; blue, MitoTracker™. Bars, 2µM

Table 1: Primers used to clone T. pseudonana sAC-like genes and corresponding nucleotide sequences

Primer name	Nucleotide sequence
Thaps3-24827 Fwd	5'-CCTCTCATAAATTATCTGATTTACCAAACCATGGGCGAGAACGGCCACTGCGGCAACGGC-3'
Thaps3-24827 Rev	5'-TCCGCTTCCAGACGTAGAACCACTCCCTTTGTTGTTGTTACTGACAAATCTTATCCCAAG-3'
Thaps3-22442 Fwd	5'-CCTCTCATAAATTATCTGATTTACCAAACCATGTCGACGGATGAAGCCGCCGGTGCCATC-3"
Thaps3-22442 Rev	5'-TCCGCTTCCAGACGTAGAACCACTCCCTTTACTACTACTGTCGGATTCGTCTAGGCAACA-3'

Table 2: Cell densities, pH measurements and TCO_2 measurements for diatom cultures from the three trials. Nd = no data collected

Trial	Experiment	Replicate	Cell density in stock culture (cells/ml)	Cell density in the experimental culture (cells/ml)	pH	TCO_2
1	KH7 Dose response	Culture A	925000	925000	8.43	4.5
2	KH7 Inhibition and Washout	Culture A	4250000	4250000	nd	nd
3	KH7 Inhibition	Culture A	930000	990000	8.83	4.4
3	KH7 Inhibition	Culture B	585000	1110000	8.66	3.8
3	KH7 Inhibition	Culture C	680000	1335000	9.02	4.6

Discussion

The goals of this thesis were to identify the subcellular localizations of two sAC-related genes, Thaps3-22442 and Thaps3-24827, in the diatom *T. pseudonana*, and to do an initial characterization about their physiological roles. By conducting this research, an additional goal was to gain experience in diatom cell culture, molecular biology, respirometry, and microscopy, which increase my chances to find a job in biotechnology. Despite the unexpected complexity of the cloning part of the project combined with the unforeseen effects of COVID-19, I was unable to achieve many of these goals.

Numerous attempts were made to tag diatom sAC-related proteins with eGFP through cloning the genes Thaps3-22442 and Thaps3-24827 into conjugation vectors. But unfortunately, this was not accomplished due to many challenges throughout the process that impeded the cloning of these genes into an expression vector. The first challenge was that the large size of these genes (Thaps3-22442 is ~5.6 kbp and Thaps3-24827 is ~6.8 kbp) greatly increased the time required to obtain products by PCRs from genomic DNA. Nonetheless, this task was eventually achieved. The next challenge was cloning the genes into the Gateway destination vectors, and this could not be achieved. Again, the most likely explanation for this failure is the large size of the genes. To avoid having to use the Gateway two-step reaction and to test the possibility of combining multiple, large DNA fragments in a single step, I switched to the Gibson cloning method. In this case, the challenge was to cut out the unnecessary gene that was already contained in the expression vector, and to isolate and amplify the backbone fragments by PCR. Attempts were made to amplify the backbone fragment as a whole piece and also as two separate pieces, however neither were successful.

Future research will continue these efforts, and once the backbone is successfully isolated and amplified, Thaps3-22442 and Thaps3-24827 could be inserted into the vector using the Gibson cloning protocol to combine these genes with the backbone containing the fcp promoter and terminator regions and the sequence coding for eGFP in frame with the genes. Once this is achieved, the bacterial-conjugation method described by Moosburner & Allen (2019) can be used to transform *T. pseudonana* cells with the expression plasmids and visualize the subcellular localizations of sAC-eGFP within *T. pseudonana*. This information will help understand the results from the O_2 measurement experiments presented in this thesis and may also provide hints for additional potential roles.

To explore a potential role of sAC in modulating *T. pseudonana* photosynthesis, I tested the effect of the small molecule KH7 on photosynthetic O_2 production. KH7 is a specific inhibitor of sAC from animals, and has been shown to abolish HCO_3^--stimulated cAMP production in *T. pseudonana* lysates (Tresguerres, 2014). KH7 inhibited *T. pseudonana* GOP rates in a dose-response manner, an effect that was partially reversible after washing out KH7 with fresh medium. This preliminary experiment provided initial evidence that a sAC-like protein (Thaps3-22442, Thaps3-24827, both, or others) are involved in regulating one or many of the mechanisms that sustain photosynthesis. However, the dose response assay involved only one replicate because of time limitations and mechanical difficulties with the O_2 electrode. The washout experiment also included only one replicate and the culture was grown in ASW instead of the F/2 medium that was used in all other experiments. These two assays should be repeated to solidify the authenticity of the results and rule out differential effects due to variations in culture conditions and growth rates.

Although 10 μM KH7 consistently inhibited GOP rate, its actual potency varied between trials: inhibition was ~90% in the first trial, but ~51% during the second and third trials. This might be explained by differential effects caused by culture conditions (ASW vs F/2 medium) or stage in the average cell cycle of the cultures. For example, the culture used in the first preliminary trial had a pH of 8.43, was lower than all three cultures used in the third trial (pH 8.66, 8.83 and 9.02) (Table 1). In addition, the density of the stock cultures A from the first trial (925,000 cells/ml) and culture A from the third trial (930,000 cells/ml) were much lower than that of culture A in the second trial (4,250,000 cells/ml), and higher than those of cultures B (585,000 cells/ml) and C (680,000 cell/ml) from the third trial. Thus, it is possible that the different cultures had cells were in different physiological stages and in which sAC was playing different roles and/or had different location of sAC within the cell. For example, cells at the exponential growth phase might have enhanced capacity for primary production compared to cells at the stationary stage of culture growth.

Although 10 μM and 20 μM KH7 induced a similar degree of GOP inhibition in the third trial, there were stark differences between the two KH7 doses in the NOP rates (3.334 ± 0.869 fmol/cell/min for 10 μM KH7 vs -0.637 ± 0.320 fmol/cell/min for 20 μM KH7) and OC rates (3.072 ± 0.738 fmol/cell/min for 10 μM KH7 vs 7.222 ± 2.602 fmol/cell/min for 20 μM KH7) as well as in the O_2 traces. Since 10 μM KH7 did not affect OC rate, the significant inhibition in NOP rates indicates an effect on photosynthetic oxygen production. I propose this effect points to the involvement of sAC in one or multiple steps of this process, which could include the regulation of CCM proteins, of proteins from photosystems I or II, of enzymes of the Calvin-Benson cycle, or combinations. However, the NOP rates for the 20 μM KH7 dosed samples behaved differently. When averaged across all three-replicate culture, the NOP rates were -0.637

fmol/cell/min. (Figure 8a) This indicates that more O_2 was being consumed than produced during the light exposure time period. In addition, the O_2 traces for the 20 μM dosed samples (Figure 11) display multiple irregularities that could be attributed to alterations to sAC-dependent regulation of mitochondrial respiration, or sAC-dependent coupling of respiration and photosynthesis. For example, some mammalian sAC isoforms can be found within mitochondria by determining the mitochondria and modulate intramitochondrial cAMP production and oxidative phosphorylation (Valsecchi et al. 2014). Future experiments should study a potential role of sAC in diatom energy metabolism. Alternatively, the results obtained with 20 μM KH7 could have been due to off-target toxic effects. In mammals, it has been shown that 30 μM and 50 μM KH7 induced a large increase in respiration in isolated brain cortex mitochondria of mice, which were attributed to mitochondrial uncoupling by KH7 independently of sAC (Jakobsen, 2018). However, the same study found that KH7 applied at ≤ 10 μM induced a reduction (or in some cases, no effect) on mitochondrial respiration and ATP production that was attributed to the inhibition of sAC. The lack of effect of 10 μM KH7 on diatom OC rates in my experiments align with those previously described in mice, adding support to the conclusion that the effect of this dose is due to specific inhibition of diatom sAC, and suggesting that the increased OC rate and irregularities seen in the O_2 traces in the 20 μM KH7 treatment might be due to off-target effects.

With the exception of cloning, all the experiments described in this thesis were performed using *T. pseudonana* expressing VHA_B-eGFP. The underlying reason is that these cells can be used to visualize the localization of VHA_B in real time in live cells based on the eGFP tag (Yee et al 2019), and VHA has been hypothesized to be an important part of the CCM through the acidification of the space between the chloroplast ER membranes and chloroplast membrane

(Lee and Krugens 1998, 2000). The VHA protein complex uses the energy from ATP hydrolysis to transports H^+ ions across cellular membranes (Nishi and Forgac, 2002). The presence of proton pumps and specifically VHA in the chloroplast membranes would pump H^+ into these internal spaces and acidify them, which would contribute to the diatom CCM. VHA isoform c" has been tagged and localized in the chloroplast ER of *P. tricornutum* (Bussard and Lopez, 2014) and a similar localization was reported for VHA isoform B in *T. pseudonana* (unpublished data by Yee et al.). In mammals and sharks, sAC has been shown to regulate H^+ transport and insertion of VHA in membranes, as well as colocalize with VHA. (Pastor-Soler et al. 2003; Gong et al, 2010; Tresguerres et al, 2010, Roa and Tresguerres, 2016). Altogether, these suggest that sAC could be regulate VHA localization and activity in relation to the diatom CCM. However, there were no discernable differences in subcellular VHA localization (visualized in VHA_B-eGFP *T. pseudonana*) between control and 10 or 20 μM KH7 treated samples. There was no visible effect on the location of VHA or other structures such as the chloroplasts or the mitochondria. However, this preliminary conclusion must be confirmed through additional experiments. This also emphasizes the importance of tagging diatom sAC proteins with eGFP, because information about their subcellular localization would provide important clues about their physiological roles.

In summary, this study confirmed the presence of the sAC-like genes Thaps3-22442 and Thaps3-24827 in the marine diatom *T. pseudonana*, and provided novel information about the potential involvement of sAC in the regulation of diatom photosynthesis. Future experimentation could explore the potential roles of sAC in regulating specific aspects of the CCM using partially inhibitory KH7 concentrations in conjunction with VHA and CA inhibitors. While the use of KH7 at higher concentrations can lead to unspecific affects and high levels disruption of crucial

mechanisms within the cell, my thesis indicated that 10 μM KH7 inhibits GOP rate without affecting OC, which suggest it acts through specifically inhibiting sAC. In addition, future research could study the potential role of sAC in regulating other key mechanisms within the photosynthetic system. Finally, the generation of diatom cell lines expressing Thaps3-22442 and Thaps3-24827 with eGFP will allow us to visualize their subcellular localizations, which is crucial for understanding the roles of these sAC-like proteins in diatom physiology.

References

Badger M.R., and Andrews T.J. (1987) CO-Evolution of Rubisco and CO_2 Concentrating Mechanisms. *Progress in Photosynthesis Research.* Springer, Dordrecht. 601-609.

Badger, M. R., Andrews, T. J., Whitney, S. M., Ludwig, M., Yellowlees, D. C., Leggat, W., & Price, G. D. (1998). The diversity and coevolution of Rubisco, plastids, pyrenoids, and chloroplast-based CO_2-concentrating mechanisms in algae. *Canadian Journal of Botany*, *76*(6), 1052-1071.

Barott K.L., Venn, A., Thies, A.B., Tabutteé, S., and Tresguerres M. (2020). Regulation of coral calcification by the acid-base sensing enzyme soluble adenylyl cyclase. *Biochem Biophys Res Comm*. *525*(3), 576-580.

Barott, K.L., Barron, M.E., and Tresguerres, M. (2017). Identification of a molecular pH sensor in coral. *Proceedings of the Royal Society B. 284*: 20171769.

Bedoshvili, Y.D., Popkova, T.P, and Likhoshway, Y.V. Chloroplast structure of diatoms of different classes. *Cell and Tissue Biology*. *3*(1), 297-310.

Bitterman, J.L., Ramos-Espiritu, L., Diaz, A., Levin, L.R., and Buck, Jochen. (2013). Pharmacological distinction between soluble and transmembrane adenylyl cyclases. *The Journal of Pharmacology and Experimental Therapeutics*. *347*(3), 589-598.

Buck, J., Sinclair, M.L., Schapal, L., Martin, J.C., and Levin, L.R. (1999). Cytosolic adenyly cyclase defines a unique signaling molecule in mammals. *Proceedings of the National Academy of Sciences USA. 96*(1), 79-84.

Bussard, A., and Lopez, P.J. (2014). Evolution of vacuolar pyrophosphatases and vacuolar H+-ATPases in diatoms. *Journal of Marine Science and Technology. 22*(1), 50-59.

Cann, M.J., Hammer, A., Zhou, J., and Kanacher, T. (2003). A defined subset of adenyly cyclases is regulated by bicarbonate ion. *Journal of Biological Chemistry. 278*(37), 35033-35038.

Carré, I.A., and Edmunds, L.N. (1993). Oscilator control of cell division in *Euglena*: cyclic AMP oscillations mediate the phasing of the cell division cycle by the circadian clock. *Journal of Cell Science*. *104*(1), 1163-1173.

Chen, Y., Cann, M. J., Litvin, T. N., Iourgenko, V., Sinclair, M. L., Levin, L. R., & Buck, J. (2000). Soluble adenylyl cyclase as an evolutionarily conserved bicarbonate sensor. *Science, 289*(5479), 625-628.

Cooper, D.M.F. (2003). Regulation and organization of adenyly cyclases and cAMP. *Biochemical Journal. 375*(3), 517-529

Darley, W.M., and Volcani, B.E. (1969). Role of silicon in diatom metabolism: A silicon requirement for deoxyribonucleic acid synthesis in the diatom *Cylindrotheca fusiformis* reimann and lewin. *Experimental Cell Research*. *58*(2-3), 334-342.

Falkowski, P., Katz, M., Knoll, A., Quigg, A., Raven, J., Schofield, O., and Taylor, F. (2004). The Evolution of Modern Eukaryotic Phytoplankton. *Science*. *305*(5682), 354-360.

Falkowski, P., Scholes, R. J., Boyle, E. E. A., Canadell, J., Canfield, D., Elser, J., Gruber, N., Hibbard, K., Högberg, P., Linder, S., Mackenzie, F.T., Moore III, B., Pedersen, T., Rosenthal, Y., Seitzinger, S., Smetacek, V., and Steffen, W. (2000). The global carbon cycle: a test of our knowledge of earth as a system. *Science*, *290*(5490), 291-296.

Falkowski, P.G., Barber, R.T., and Sametacek, V. (1998). Biogeochemical controls and feedbacks on ocean primary production. *Science*, *281*(5374), 200-206

Field, C.B, Behrenfeld, M.J., Randerson, J.T., and Falkowski, P. (1998). Primary production of the biosphere: integrating terrestrial and oceanic components. *Science, 281*(5374), 237-240.

Gentil, J., Hempel, F., Moog, D., Zauner, S., and Maier, U.G. (2017). Review: origin of complex algae by secondary endosymbiosis: a journey through time. *Protoplasma. 254*(1), 1835-1843

Gibbs, S.P. (1979). The route of entry of cypoplasmically synthesized proteins into chloroplast or algae possessing chloroplast ER. *Journal of Cell Science, 35*(1), 253-266.

Gong, F., Alzamora, R., Smolak, C., Li, H., Naveed, S., Neuman, D., Hallows, K.R., and Pastor-Soler, N.M. (2010). Vacuolar H^+-ATPase apical accumulatio in kidney intercalated cells is regulated by PKA and AMP-activated protein kinase. *American Journal of Physiology Renal Physiology 298*: F1162–F1169

Guillard, R.L, and Ryther, J.H. Studies of marine planktonic diatoms: I. *Cyclotella nana Hustedt* and *Detonula confervacea* (Cleve) Gran. *Canadian Journal of Microbiology*, *8*(2), 229-239

Harada, H., Nakajima, K., Sakaue, K., & Matsuda, Y. (2006). CO_2 sensing at ocean surface mediated by cAMP in a marine diatom. *Plant Physiology*, *142*(3), 1318-1328.

Hennon, G. M., Ashworth, J., Groussman, R. D., Berthiaume, C., Morales, R. L., Baliga, N. S., ... & Armbrust, E. V. (2015). Diatom acclimation to elevated CO_2 via cAMP signaling and coordinated gene expression. *Nature Climate Change*, *5*(8), 761-765.

Hess, K. C., Jones, B. H., Marquez, B.H., Chen, Y., Ord, T. S., Kamenetsky, M., Miyamoto, C., Zippin, J.H., Kopf, G.S., Suarez, S.S., Levin, L.R., Williams, C.J., Buck, J., and Moss, S.B. (2005). The "soluble" adenylyl cyclase in sperm mediates multiple signaling events required for fertilization. *Developmental cell*, 9(2), 249-259.

Hopkinson, B. M. (2014). A chloroplast pump model for the CO_2 concentrating mechanism in the diatom Phaeodactylum tricornutum. *Photosynthesis Research*, *121*(2-3), 223-233.

Iseki, M., Matsunaga, S., Murakami, A., Ohno, K., Shiga, K., Yoshida, K., Sugai, M., Takahashi, T., Hori, T., and Watanabe, M. (2002). A blue-light-activated adenylyl cylase mediates photoavoidance in *Euglena gracilis*. *Nature*. *415*(1), 1047-1051

Jakobsen, E., Lange, S. C., Andersen, J. V., Desler, C., Kihl, H. F., Hohnholt, M. C., ... & Bak, L. K. (2018). The inhibitors of soluble adenylate cyclase 2-OHE, KH7, and bithionol compromise mitochondrial ATP production by distinct mechanisms. *Biochemical Pharmacology*, *155(*1): 92-101.

Karas, B.J., Diner, R.E., Lefebvre, S.C., McQuaid, J., Phillips, A.P.R., Noddings, C.M., Brunson, J.K., Valas, R.E., Deerinck, T.J., Jablanovic, J., Gillard, J.T.F., Beeri, K., Ellisman, M.H., Glass, J.I., Hutchison III, C.A., Smith, H.O., Venter, J.C., Allen, A.E., Dupont, C.L., and Weyman, P.D. (2015). Designer diatom episomes delivered by bacterial conjugation. *Nature Communications. 6*(6925), 1-10

Keeling, P.J. Chromalveolates and the evolution of plastids by secondary endosymbiosis. *Journal of Eukaryotic Microbiology. 56*(1), 1-8.

Kleinboelting, S., Diaz, A., Moniot, S., van den Heuvel, J., Weyand, M., Levin, L.R., Buck, J., and Steegborn, C. (2014) Crystal structures of human soluble adenylyl cyclase reveal mechanisms of catalysis and its activation through bicarbonate. *Proceedings of the National Academy of Science USA*. *111*(10), 3727-3732

Kobayashi, M., Buck, J., and Levin, L.R. (2004). Conservation of functional domain structure in bicarbonate-regulated 'soluble' adenylyl cyclases in bacteria and eukaryotes. *Developmental Genes & Evolution. 214*:503-509

Lee, R.E., and Kugren, P. (2000). Ancient atmospheric CO_2 and the timing of evolution of secondary endosymbiosis. *Phycologia*. *39*(2), 167-172.

Lee, R.E., and Kugrens, P. (1998). Hypothesis: The ecological advantage of chloroplast ER – The ability to outcompete at low dissolved CO_2 concentrations. *Protist. 149*(4), 341-345

Linder, J.U., and Shultz, J.E. (2003). The class III adenyly cyclases: multi-purpose signalling modules. *Cellular Signaling*. *15*(1), 1081-1089

Litvin, T.N., Kamenetsky, m., Zarifyan, A., Buck, J., and Levin, L.R. (2003). Kinetic properties of "soluble" adenylyl cyclase. *Journal of Biological Chemistry. 278*(18): 15922-15926

Lo, M., Shahriari, A., Roa, J.N., Tresguerres, M., and Farrell, A.P. (2020). Differential effects of bicarbonate on severe hypoxia and hypercapnia-induced cardiac malfunctions in diverse fish species. *Journal of Comparative Physiology B.*

Matsuda, Y., Hopkinson, B. M., Nakajima, K., Dupont, C. L., & Tsuji, Y. (2017). Mechanisms of carbon dioxide acquisition and CO_2 sensing in marine diatoms: a gateway to carbon metabolism. *Philosophical Transactions of the Royal Society B: Biological Sciences*, *372*(1728), 20160403.

Matsuda, Y., Nakajima, K., & Tachibana, M. (2011). Recent progresses on the genetic basis of the regulation of CO 2 acquisition systems in response to CO_2 concentration. *Photosynthesis Research*, *109*(1-3), 191-203.

Moosburner, M., and Allen, A. (2019). CRISPR-Cas9 episome conjugation into Phaeodactylum tricornutum V.2. *Frontiers of Microbiology.* Protocols.io.

Nakajima, K., Tanaka, A., & Matsuda, Y. (2013). SLC4 family transporters in a marine diatom directly pump bicarbonate from seawater. *Proceedings of the National Academy of Sciences*, *110*(5), 1767-1772.

Nishi, T., and Forgac, M. (2002). The vacuolar (H^+) -ATPases- nature's most versatile proton pumps. *Nature Reviews Molecular Cell Biology. 3*(1), 94-103

Pastor-Soler, N., Beaulieu, V., Litvin, T.N., Da Silva, N., Chen, Y., Brown, D., Buck, J., Levin, L.R., and Breton, S. (2003). Bicarbonate-regulated adenyly cyclase (sAC) is a sensor that regulates pH-dependent V-ATPase recycling. *Journal of Biological Chemistry. 278*(49), 49523-49529

Roa, J.N., and Tresguerres, M. (2016). Soluble adenylyl cyclase is an acid/base sensor in epithelial base-secreting cells. *American Journal of Physiology Cell Physiology. 311*(1), 340-349.

Salmerón, C., Harter, T.S., Kwan, G.T., Roa, J.N., Blair, S.D., Rummer, J.L., Shiels, H.A., Goss, G.G., Wilson, R.W., and Tresguerres M. (2021). Molecular and biochemical characterization of the bicarbonate-sensing soluble adenylyl cyclase from a bony fish, the rainbow trout *Oncorhynchus mykiss*. *Interface Focus*

Samukawa, M., Shen, C., Hopkinson, B. M., & Matsuda, Y. (2014). Localization of putative carbonic anhydrases in the marine diatom, Thalassiosira pseudonana. *Photosynthesis Research*, *121*(2-3), 235-249.

Steegborn, C. (2014). Structure, mechanism and regulation of soluble adenylyl cyclases—similarities and differences to transmembrane adenylyl cyclases. *Biochimica et Biophysica Acta. 1842*(12), 2535-2547.

Stoebe, B. and Maier, U.G. (2002). One, two, three: nature's tool box for building plastids. *Protoplasma*. *219*(1), 123-130

Tachibana, M., Allen, A. E., Kikutani, S., Endo, Y., Bowler, C., & Matsuda, Y. (2011). Localization of putative carbonic anhydrases in two marine diatoms, Phaeodactylum tricornutum and Thalassiosira pseudonana. *Photosynthesis Research*, *109*(1-3), 205-221.

Tcherkez, G.G.B., Farquhar, G.D., and Andrews T.J. (2006) Despite slow catalysis and confused substrate specificity, all ribulose bisphosphate carboxylases may be nearly perfectly optimized. *Proceedings of the National Academy of Sciences*, *103*(19), 7246–7251

Tresguerres, M. (2014). sAC from aquatic organisms as a model to study the evolution of acid/base sensing. *Biochimica et Biophysica Acta (BBA)-Molecular Basis of Disease*, *1842*(12), 2629-2635.

Tresguerres, M., Barott, K. L., Barron, M. E., & Roa, J. N. (2014). Established and potential physiological roles of bicarbonate-sensing soluble adenylyl cyclase (sAC) in aquatic animals. *Journal of Experimental Biology*, *217*(5), 663-672.

Tresguerres, M., Levin, L.R., and Buck, J. (2011). Intracellular cAMP signaling by soluble adenyly cyclase. *International Society of Nephrology. 79*(12), 1277-1288.

Tresguerres, M., Parks, S.K., Salazar, E., Levin, L.R., Goss, G.G., and Buck, J. (2010). Bicarbonate-sensing soluble adenyly cyclase is an essential sensor for acid/base homeostasis. *Proceedings of the National Academy of Sciences USA. 107*(1), 442-447

Valsecchi, F., Konrad, C., and Mafredi, Giovanni. (2014). Role of soluble adenyl cyclase in mitochondria. *Biochimica et Biophysica Acta. 1842*(1), 25555-2560.

Yee, D., Hildebrand, M., and Tresguerres, M. (2019). Dynamic subcellular translocation of V-type H^+ -ATPase is essential for biomineralization of the diatom silica cell wall. *New Phytologist. 225*(6), 1-12

Yool, A., and Tyrrel, T. (2003). Role of diatoms in regulating the ocean's silicon cycle. *Global Biogeochemical Cycles, 17*(4), 1-21.

Yoon, H.S., Hackett, J.D., Pinto, G., and Bhattacharya, D. (2002). The single, ancient orgin of chromist plastids. *Proceedings of the National Academy of Science USA. 99*(24), 15507-12

Zippin, J.H., Chen, Y., Nahirney, P., Kamenetsky, M., Wuttke, M.S., Fischman, D.A, Levin, L.R., and Buck, J. (2002). Compartmentalization of bicarbonate-sensitive adenylyl cyclase in distinct signaling microdomains. *The FASEB Journal*. *17*(1), 1-15

Zippin, J.H., Farrell, J., Huron, D., Kamenetsky, M., Hess, K.C., Fischman, D.A., Levin, L.R., and Buck, J. (2004). Bicarbonate-responsive "soluble" adenylyl cyclase defines a nuclear cAMP microdomain. *The Journal of Cell Biology*. *164*(4), 527-534.